



저작자표시-비영리-변경금지 2.0 대한민국

이용자는 아래의 조건을 따르는 경우에 한하여 자유롭게

- 이 저작물을 복제, 배포, 전송, 전시, 공연 및 방송할 수 있습니다.

다음과 같은 조건을 따라야 합니다:



저작자표시. 귀하는 원저작자를 표시하여야 합니다.



비영리. 귀하는 이 저작물을 영리 목적으로 이용할 수 없습니다.



변경금지. 귀하는 이 저작물을 개작, 변형 또는 가공할 수 없습니다.

- 귀하는, 이 저작물의 재이용이나 배포의 경우, 이 저작물에 적용된 이용허락조건을 명확하게 나타내어야 합니다.
- 저작권자로부터 별도의 허가를 받으면 이러한 조건들은 적용되지 않습니다.

저작권법에 따른 이용자의 권리는 위의 내용에 의하여 영향을 받지 않습니다.

이것은 [이용허락규약\(Legal Code\)](#)을 이해하기 쉽게 요약한 것입니다.

[Disclaimer](#)

수의학석사학위논문

개의 결손골 모델에서
자가혈청유래 알부민 스캐폴드와
개 지방유래 간엽줄기세포의
골 형성 촉진

**Effect of serum-derived albumin scaffold and
canine adipose tissue-derived mesenchymal stem cells on
osteogenesis in canine segmental bone defect model**

2014 년 2 월

서울대학교 대학원
수의학과 수의외과학 전공
윤 대 영

개의 골결손 모델에서 자가혈청유래 알부민 스캐폴드와 개 지방유래 간엽줄기세포의 골 형성 촉진

**Effect of serum-derived albumin scaffold and
canine adipose tissue-derived mesenchymal stem cells on
osteogenesis in canine segmental bone defect model**

지도교수 권 오 경

이 논문을 수의학석사학위논문으로 제출함
2013 년 10 월

서울대학교 대학원
수 의 학 과 수 의 외 과 학 전 공
윤 대 영

윤대영의 석사학위논문을 인준함.
2013 년 12 월

위 원 장 김 완 희 (인)

부위원장 권 오 경 (인)

위 원 김 대 용 (인)

Effect of serum-derived albumin scaffold and canine adipose tissue-derived mesenchymal stem cells on osteogenesis in canine segmental bone defect model

Supervisor: Professor Oh-Kyeong Kweon

Daeyoung Yoon

Major in Veterinary Surgery

Department of Veterinary Medicine

Graduate School of Seoul National University

Abstract

Composite synthetic grafts with progenitor cells instead of auto or allografts offer an alternative approach for the fracture repair. The aim of this study was to evaluate osteogenesis of autologous serum-derived albumin (ASA) scaffold seeded with canine adipose tissue-derived mesenchymal stem cells (Ad-MSCs) in canine segmental bone

defect model. ASA scaffold was prepared with canine serum by cross-linking and freeze-drying procedures. Beta-tricalcium phosphate (β -TCP) was mixed at cross-linking stage of the procedures. Ad-MSCs were seeded into scaffold and incubated for a day before implantation. The grafts were harvested 16 weeks after implantation for histological analysis. Dogs were divided into five groups; control, ASA scaffolds with and without Ad-MSCs, ASA scaffolds including β -TCP with and without Ad-MSCs. The group of ASA scaffold with Ad-MSCs had larger radiopaque area on radiographs than the groups with β -TCP and more bone formation in histological finding than other groups ($p < 0.05$). It was suggested that Ad-MSCs seeded into ASA scaffold enhanced osteogenesis in bone defect model but β -TCP in the ASA scaffold prevented the penetration of the cells related to bone healing. However, more time is required to verify whether fibrous tissues in the middle of the defects could be converted to osteoprogenitor cells.

Keywords: Adipose-derived mesenchymal stem cells, Bone defect, Serum-derived albumin scaffold

Student Number: 2011-21673

CONTENTS

I.	INTRODUCTION	1
II.	MATERIALS AND METHODS	3
1.	AUTOLOGOUS SERUM-DERIVED ALBUMIN SCAFFOLDS	3
2.	PREPARATION OF BETA-TRICALCIUM PHOSPHATE (β -TCP)	4
3.	PREPARATION OF CANINE ADIPOSE-DERIVED MESENCHYMAL STEM CELLS	4
4.	CELL SEEDING	5
5.	ORTHOTOPIC IMPLANTATION AND HARVEST	6
6.	RADIOGRAPHIC EXAMINATION	9
7.	HISTOLOGICAL EXAMINATION	9
8.	STATISTICAL ANALYSIS	10
III.	RESULTS	11
1.	RADIOGRAPHIC FINDINGS	11
2.	HISTOLOGICAL FINDINGS	15
IV.	DISCUSSION	21
V.	REFERENCES	25
VI.	ABSTRACT IN KOREAN	31

I. Introduction

The repair of large segmental defects in diaphyseal bone is a challenge to veterinary clinics. The use of autologous bone graft or allograft has been viewed as the historical standard of treatment (Drosse et al. 2008) but is associated with substantial morbidity including infection, disease transmission, and loss of function (Aho et al. 1994, Ehrler et al. 2000, Garbuz et al. 1998, Head et al. 1999). The complications resulting from graft harvest and the limited supply have inspired the development of alternative strategies for the repair of clinically significant bone defects. The primary approach to this problem has focused on the development of biological or synthetic implant materials and using mesenchymal stem cells (MSCs) (Drosse et al. 2008).

MSCs are multipotent cells derived from bone marrow, adipose tissue, muscle, umbilical cord blood, and the placenta, which are capable of differentiating into myoblasts, tenocytes, chondrocytes, and adipocytes (Drosse et al. 2008, Pittenger et al. 1999). Also, MSCs are capable of differentiating along the osteoblastic lineage. Previously, we isolated and characterized the MSCs derived from the adipose tissues of dogs (Ryu et al. 2009). Canine adipose tissue-derived MSCs (Ad-MSCs) have an ability to differentiate into osteoblasts and clear advantages including easy and repeatable access to subcutaneous adipose tissue; a

simple isolation procedure; abundance in supply; and a relatively noninvasive harvesting procedure (Schäffler et al. 2007).

Synthetic bone substitutes and materials containing the osteogenic potential have been evaluated as scaffold material (Arinzeh et al. 2005, Tseng et al. 2008). Among the synthetic bone substitutes, beta tricalcium phosphate ceramics have shown the most promising results due to their osteoconductive properties, unlimited availability, and absence of immune response (Oonishi 1991, Sartoris et al. 1992). Moreover, Ad-MSCs mixed with beta-tricalcium phosphate have osteogenic potential in ectopic implantation (Byeon et al. 2010).

In order to support cell growth and control osteogenic differentiation, appropriate scaffolds are essential in bone tissue engineering. For cell scaffolding, the ideal scaffolds would be a highly porous material with good biocompatibility and osteointegrative properties (Hutmacher 2000, Salgado et al. 2004). Serum-derived scaffolds have reported to possess great scaffolding potential due to their biological porosity structure and high seeding efficiency (Gallego et al. 2010). In addition, we showed that the combination of collagen I gel enhanced osteogenic differentiation and homogenous distribution of Ad-MSCs seeded onto ASA scaffold (Kang et al. 2013).

In this study, we evaluated the osteogenic potential of the canine ASA scaffold mixed with or without β -TCP and seeded with or without Ad-MSCs in the bone defect model of dogs.

II. Materials and Methods

1. Autologous serum-derived albumin scaffolds

Autologous serum-derived albumin scaffolds were fabricated according to the freeze-drying and chemical cross-linking procedures (Gallego et al. 2010, Gallego et al. 2010). Briefly, 10 ml canine venous blood was taken by venipuncture and kept at 37°C for 30 min to retract fibrin clot. Next, the blood sample was centrifuged at 3000 rpm for 15 min to obtain serum, and then 0.5 ml glutaraldehyde 25% solution (Sigma-Aldrich, St. Louis, MO, U.S.A.) was added to 5 ml of serum obtained from the cross-linking. The serum mixed with glutaraldehyde solution was transferred to 1 ml disposable syringe and was kept until solidification. Then, the solution was moved to the freezing machine and maintained at -70°C overnight. After cutting the syringe, the cross-linked frozen solution was lyophilized for 48 hr in a freeze dryer (DFU-8603, Operon). After that, the cylindrical sponge was obtained and rehydrated in graded ethanol series (100%, 90% and 80%) by dipping in each one for 1 hr. The obtained scaffold was cut into 20-mm-length column and then sterilized in 70% ethanol for 8 hr. Lastly, the scaffold was neutralized in serum-free Dulbecco's Modified Eagle's Medium (DMEM; Gibco, Billings, MT, U.S.A.). Excess fluid was removed before cell seeding and the column-shaped scaffolds were placed in a 6-well plate (Nunc) as one scaffold

per well.

In the groups with β -TCP added, 5 ml of obtained serum was added and mixed with 0.5 ml glutaraldehyde 25% solution and 300 mg of β -TCP at once. Then, it was transferred to 1 ml disposable syringe and rolled until solidification. The latter procedures were the same as above.

2. Preparation of beta-tricalcium phosphate (β -TCP)

Beta tri-calcium phosphates granules with particle size between 200 and 300 μ m were kindly provided by the Biomaterial Center, National Institute for Material Science, Tsukuba, Japan (Kikuchi et al. 2004).

3. Preparation of canine Ad-MSCs

Canine Ad-MSCs were obtained by culturing to facilitate the proliferation of mononucleated cells from adipose tissues according to the methods described in our previous article (Kang et al. 2012). Briefly, adipose tissues were aseptically collected from the gluteal region of a 2-year-old beagle dog under general anesthesia. The adipose tissues were extensively washed with phosphate buffered saline (PBS) and then minced with scissors. The minced tissues were digested with 1 mg/ml collagenase type I (Sigma-Aldrich, St. Louis, MO,

U.S.A.) for 2 hr at 37°C. The tissue samples were washed with PBS and centrifuged at 1000 rpm for 10 min. The resulting pellet of stromal vascular fraction was resuspended, filtered through a 100 µm nylon mesh, and incubated overnight in Dulbecco's Modified Eagle's Medium (DMEM; Gibco, Billings, MT, U.S.A.) with 10% fetal bovine serum (FBS; Gibco, Billings, MT, U.S.A.) at 37°C in a 5% CO₂ humidified atmosphere. After 24 hr, unattached cells and residual on adherent red blood cells were removed by washing with PBS. The medium was replaced every 48 hr until the cells became confluent. After cells reached 90% confluence, they were subcultured. At passage 3, these cells were used for seeding into the scaffolds.

4. Cell seeding

A suspension of 1×10^6 cells in 50 µl PBS was mixed with 250 µl purified bovine collagen solution (Nutragen®, Advanced BioMatrix) in order to improve the cellular-adherent properties of the scaffolds and increase the rate of MSC-mediated bone formation (Kang et al. 2013). They were seeded into the scaffolds placed in wells of a 6-well plate and incubated in the growth medium (DMEM supplemented with 10% FBS) at 37°C and 5% CO₂ for a day before implantation in vivo.

5. Orthotopic implantation and harvest

All animal procedures were performed in accordance with the guidelines of the Institutional Animal Care and Use Committee of Seoul National University (SNU-121217-1). Ten skeletally mature beagle dogs (average weight, 8.95 ± 0.96 kg and average age 1.3 ± 0.5 years) were used for the orthotopic implantation. The segmental resection of part of the ulna was performed bilaterally as described previously (Nilsson et al. 1986). The dogs were sedated with an intravenous injection of acepromazine maleate (Sedaject, Samwoo Medical, Yesan, South Korea) at a dose of 0.01 mg/kg of body weight and were premedicated with an subcutaneous injection of atropine sulfate (Jeil Pharmaceutical, Daegu, South Korea) at a dose of 0.1 mg/kg of body weight. Anesthesia then was induced by intravenous administration of a mixture of zolazepam/tiletamine (25 mg/ml; Zoletil 50® , Virbac Korea, Seoul, South Korea) at a dose of 5 mg/kg of body weight and maintained with isoflurane (Aerrane, Baxter, Mississauga, ON, Canada) in oxygen. Intravenously administered tramadol (Toranzin®, Samsung Pharmaceutical, Seoul, South Korea) and cefazolin (Samsung Pharmaceutical, Seoul, South Korea) at a dose of 4 mg/kg and 22 mg/kg of body weight were used as an analgesic and antibiotics, respectively. Anesthesia monitor (Datex-Ohmeda; Microvitec Display, UK) was used to monitor physiologic factors including rectal temperature, oxygen saturation, end tidal CO₂, electrocardiogram, minimum alveolar concentration value, and

pulse rate. Under sterile conditions, a caudal approach was performed to expose the diaphysis of ulna. The overlying periosteum was resected from the defect area. The eight-hole, 5.0 X 42-mm dynamic compression plate (Synthes, Switzerland) was contoured and applied to the medial aspect of the ulna. The plate was then removed and a 15 mm long osteoperiosteal segmental cortical defect was made at the mid-portion of the diaphysis with an oscillating saw (Stryker, USA) (Fig. 1b). The defect was filled with autologous serum-derived albumin scaffold (Alb, n=4), albumin scaffold seeded with Ad-MSCs (Alb + Ad-MSCs, n=4), albumin mixed with β -TCP scaffold (Alb + β -TCP, n=4), albumin mixed with β -TCP scaffold plus Ad-MSCs (Alb + β -TCP + Ad-MSCs, n=4), or nothing (control, n=4) (Fig. 1c). The plate was then reapplied, and the prepared scaffolds were implanted in the defect. Each dog received an implant on each ulna randomly. After closing the soft tissue, a Robert John's bandage was applied for 2 weeks. Two weeks after surgery, all animals were active, fully able to walk, and bearing weight. The implants were harvested 16 weeks after implantation and used for histological examinations (Fig. 1d).

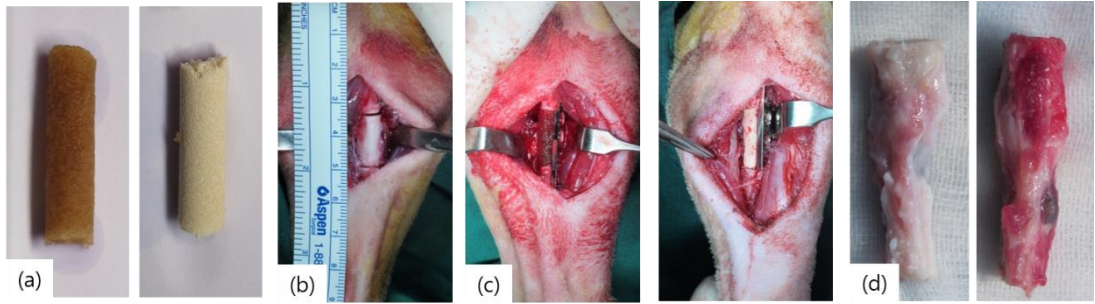


Fig. 1. The orthotopic implantation procedure. (a) Scaffold preparation; Left, serum-derived albumin scaffold. Right, serum-derived albumin scaffold mixed with β -tricalcium phosphate (β -TCP). (b) Segmental defect in the ulnar diaphysis. (c) Filling the bone defect with scaffold; Left, serum-derived albumin scaffold mixed with β -tricalcium phosphate (β -TCP). Right, serum-derived albumin scaffold. (d) Implant harvested after 16 weeks.

6. Radiographic examination

Lateral and craniocaudal radiographs of the antebrachium were made before and immediately after surgery as well as 4, 8, and 16 weeks after implantation. All of the radiographs assessed the total area of new bone formation at the proximal and distal host cortex-implant interfaces. Radiographic imaging software (Inifnitypacs®, INFINITT healthcare Co., Korea) was used to measure the area occupied by new bone formation.

7. Histological examination

A 5-cm segment of bone including the defect site was harvested and fixed in 4% paraformaldehyde. The samples were decalcified with hydrochloric acid, dehydrated in a series of ethanol solutions, and embedded longitudinally in paraffin. The samples were cut in the sagittal plane. The central longitudinal sections from each ulna were placed on the ground to a thickness of 100 μm and stained with hematoxylin and eosin (H&E), and Masson's trichrome stains to evaluate new bone formation.

Stained sections from each group were observed under a light microscope and were scanned using an attached digital camera and a NIS-Elements system (Nikon, Japan). For histomorphometric analysis, all groups were analyzed according to the following protocol. The entire implant area was viewed in six microscopic fields. Each field was captured using

a digital camera and was subjected to histomorphometric analyses. Interface between new bone and host bone in the histological picture was marked by measuring the distance from the screw hole in the radiographs. Area of the newly formed bone area (NBA) were estimated and converted into a percentage of the total implanted area (TA) using an image processing and analysis software (ImageJ; National Institutes of Health, USA).

8. Statistical Analysis

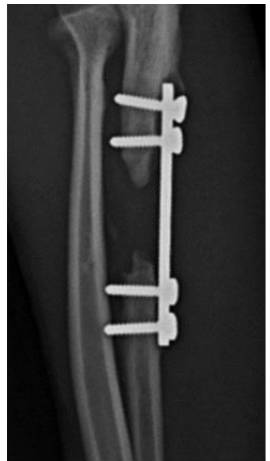
Data were analyzed using SPSS statistical analytical software (ver. 18.0; SPSS Inc. DE, USA). Significant differences in radiographic examination were detected over time with one-way analysis of variance. A Kruskal-Wallis test was used to assess differences among the groups. A post-hoc test was performed along with a Mann-Whitney U test. P-value less than 0.05 were considered to be statistically significant.

III. Results

1. Radiographic findings

Postoperatively, the defect could be visualized easily because of the radiopacity of the β -TCP particles (Fig. 2D and E). In all groups, reactive bone formation at transverse cut edges of the host ulnar was observed at 4 weeks. By 16 weeks, slightly more bone was present within the gap, especially along the scaffold in all the groups except control. In the control group, similar changes were only limited to areas near the interface with the host bone (Fig. 2A).

Radiomorphometric analysis showed that all treated group had significantly larger area of increased opacity at the proximal and distal host cortex-implant interfaces comparing to control groups ($p < 0.05$). In addition, the groups with β -TCP showed smaller area of increased opacity changes within bone defect space than the Alb + Ad-MSCs group ($p < 0.05$) (Table 1.).



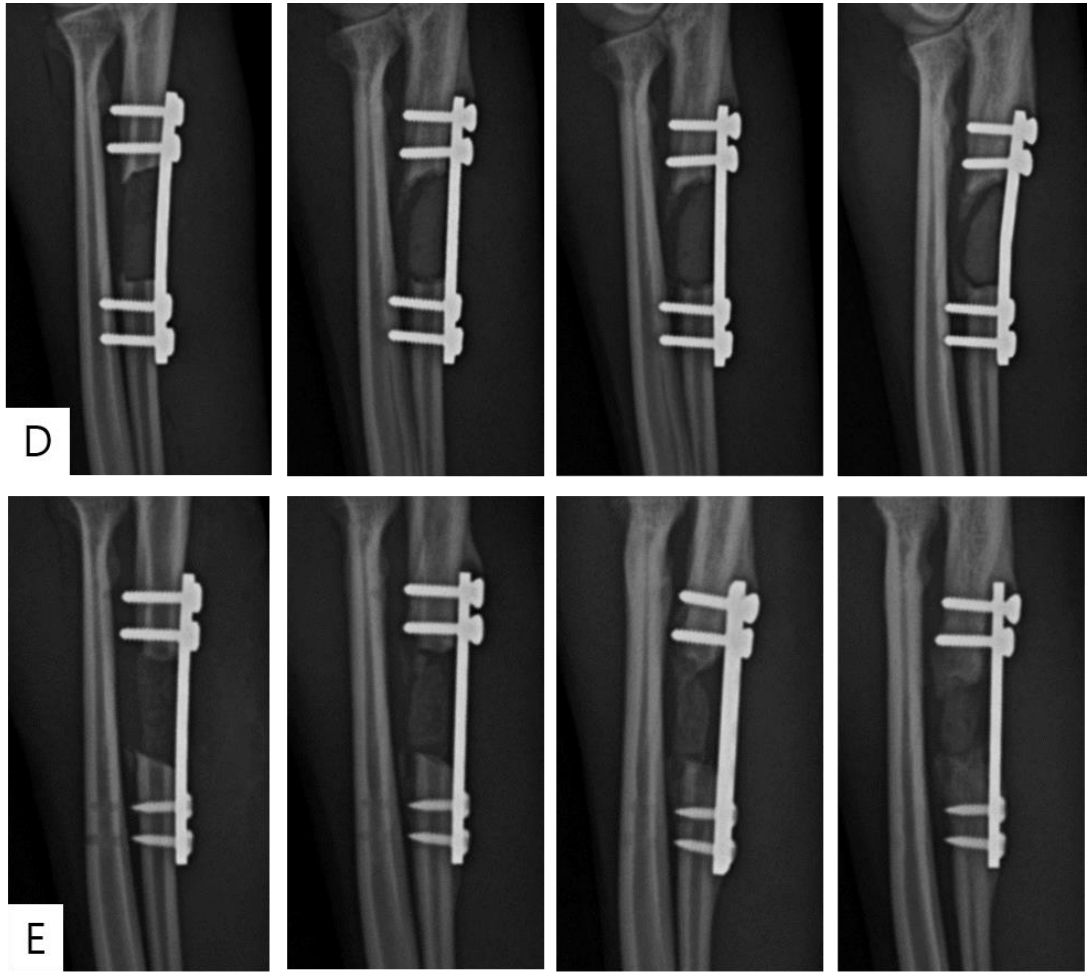


Fig. 2. Mediolateral radiographs of the treated defects obtained immediately after the operation as well as 4, 8, and 16 weeks after surgery, respectively from the left. The radiopacity area near proximal and distal host-implant interfaces in each group had changed in the periodical order. The β -TCP remained in the middle section of the defect (D and E). Control (A), Alb (B), Alb + Ad-MSCs (C), Alb + β -TCP (D), and Alb + β -TCP + Ad-MSCs (E) groups.

Table 1. Radiomorphometric analysis of the total area (mm²) of new bone formation at the proximal and distal host cortex-implant interfaces at 4, 8, and 16 weeks after implantation.

Groups	4 weeks after implantation	8 weeks after	16 weeks after
Control	4.90± 2.23	5.57 ± 2.25	6.48 ± 2.40 [†]
Alb	4.16 ± 2.04	10.08 ± 4.86	15.33 ± 5.21 [*]
Alb + Ad-MSCs	5.47 ± 2.62	10.64 ± 3.63	19.43 ± 3.45 [*]
Alb + β-TCP	3.57 ± 2.30	5.84 ± 2.40	10.29 ± 3.37 ^{*†}
Alb + β-TCP + Ad-MSCs	4.60 ± 2.17	6.63 ± 2.50	11.51 ± 3.62 ^{*†}

Data are presented as the mean ± SD. * significant difference (p< 0.05) compared to the control.

† significant difference (p <0.05) compared to the Alb + Ad-MSCs group.

2. Histological findings

In all experimental groups, new bone formation was observed in longitudinal sections throughout the segmental bone defect at 16 weeks after implantation. No adverse host response had been detected at histological findings. Histologically, newly formed bone was primarily observed on the cortex-implant interfaces, especially the proximal part. Most of the areas at the middle section of the implant were filled with fibrous connective tissue (Fig. 3). Grossly, the β -TCP applied group showed that β -TCP remained in the middle section of the defect (Fig. 3 and 4). ASA + Ad-MSCs group showed chondrocytic change and new woven trabecular bone formation (Fig. 4)

The bone formation capacity was assessed in all groups by measuring areas of newly formed bone on histological image (Fig. 3). Percentage of new bone formation to total area was significantly higher for all treated group compared to control group ($p < 0.05$). Histomorphometric analysis was consistent with visual scoring, confirming that Alb + Ad-MSCs group had significantly greater amount of bone formation at implant to host bone interfaces than Alb group ($p < 0.05$). Moreover, Alb + Ad-MSCs group showed significantly larger area of bone formation than Alb + β -TCP and Alb + β -TCP + Ad-MSCs group ($p < 0.05$).

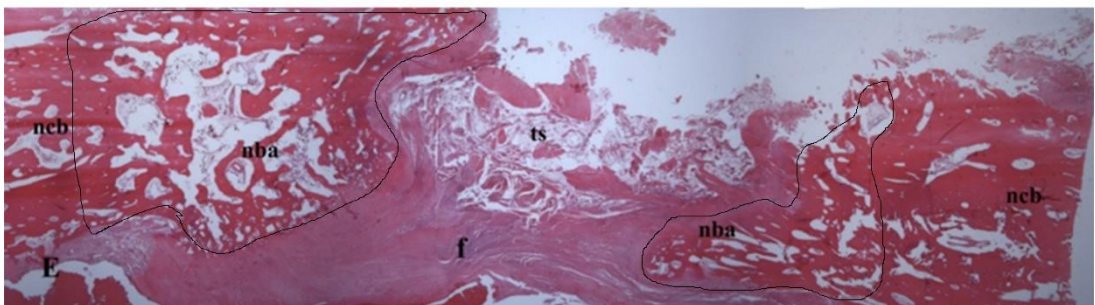
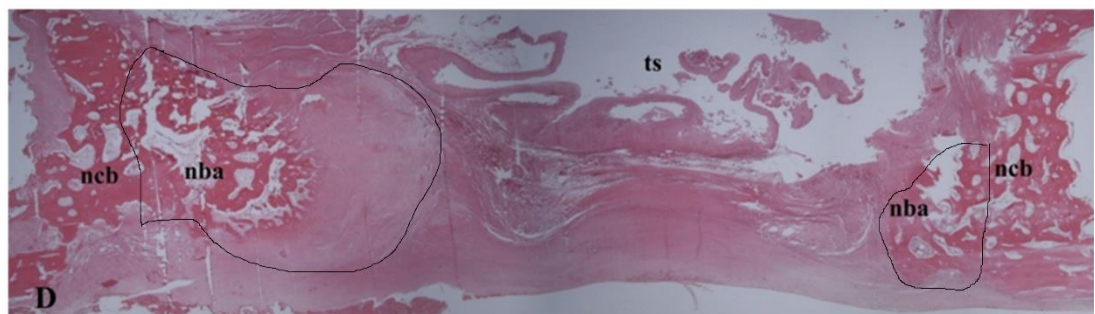
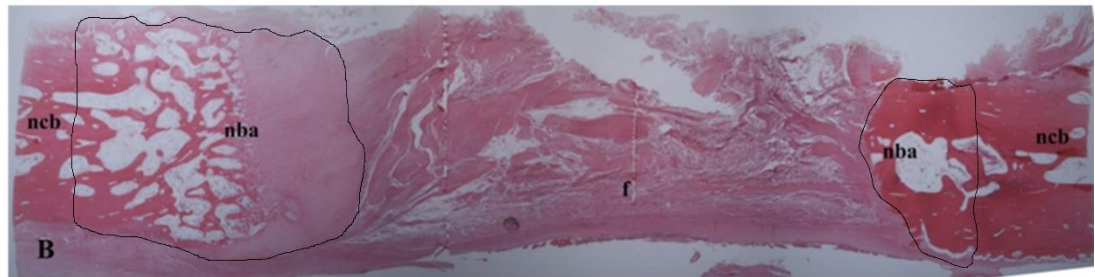
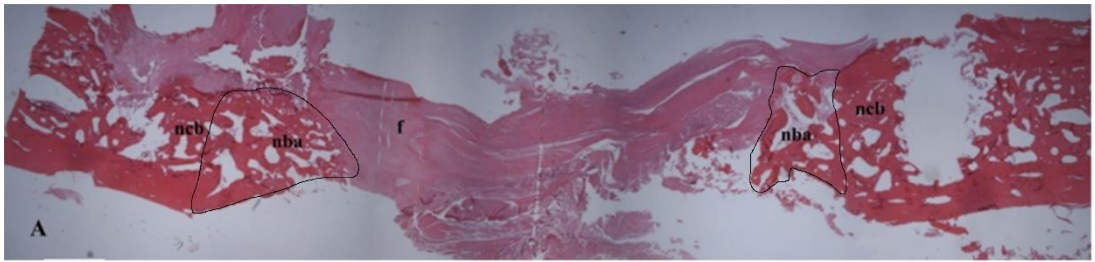


Fig. 3. Histological findings in the longitudinal sections of the segmental bone defects 16 weeks after implantation. The merged picture of whole defect area including nearby normal bone areas in each group are shown: A, Control; B, Alb; C, Alb + Ad-MSCs; D, Alb + β -TCP; E, Alb + β -TCP + Ad-MSCs groups. The proximal portion is the left of the panels (A ~ E). There was a higher amount of bone formation in all experimental groups compared to the control group. H & E stain. (ncb; native cortical bone area, nba; newly formed bone area, f; fibrous tissue, ts; serum-derived albumin scaffold mixed with β -TCP)

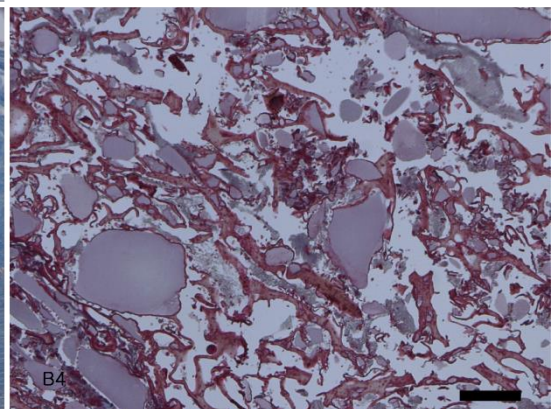
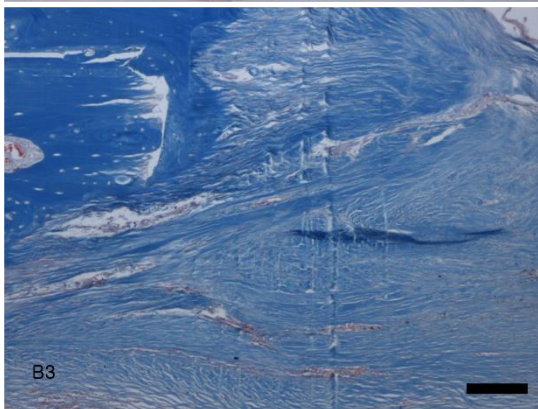
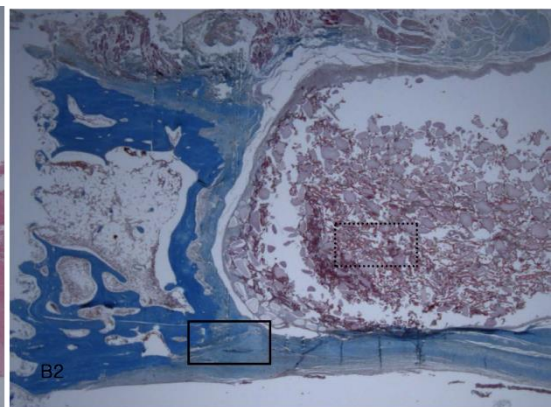
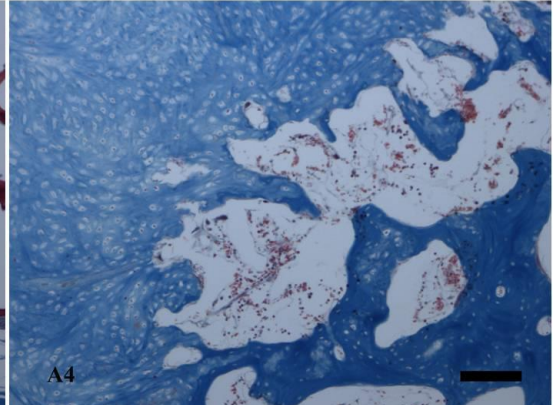
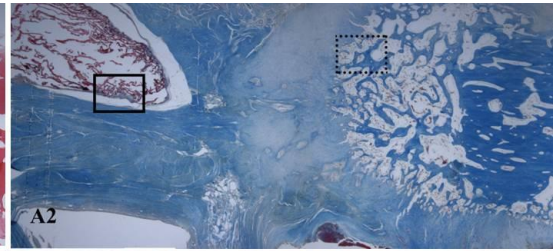


Fig. 4. Histological findings in the longitudinal sections of the interfacial area between bone defect and host bone 16 weeks after implantation. A, Alb + Ad-MSCs; B, Alb + Ad-MSCs + β -TCP groups. Merged picture of the defect area including interfacial areas and implanted scaffold (A2 and B2). Remained ASA scaffold (A3), chondrocytic change and new woven bone formation (A4), fibrous tissue (B3) were observed. Remained ASA scaffold mixed with β -TCP (B4) was observed. H & E stain (A1 and B1) and Masson's trichrome stain (A2, A3, A4, B2, B3, and B4). A3 (solid frame) and A4 (dot frame) detailed view of the A2 (x 100). B3 (solid frame) and B4 (dot frame) detailed of the B2 (x 40). (A3 and A4) and (B3 and B4) the bar represents 200 μ m and 400 μ m, respectively.

Table 2. Histomorphometric analysis of new bone formation at the proximal and distal host cortex-implant interfaces at 16 weeks after implantation

Group	NBA/TA (%)
Control	$13.30 \pm 3.11^{\dagger}$
Alb	$29.78 \pm 3.98^{*\dagger}$
Alb + Ad-MSCs	$36.07 \pm 5.72^*$
Alb + TCP	$22.83 \pm 3.21^{*\dagger}$
Alb + TCP + Ad-MSCs	$23.37 \pm 4.54^{*\dagger}$

Data are presented as the mean \pm SD. * Indicates a statistically significant difference ($p < 0.05$) compared to the control. \dagger Indicates a statistically significant difference ($p < 0.05$) compared to the Alb + Ad-MSCs group. NBA: newly formed bone area, TA: total implanted area

IV. Discussion

The objective of this study was to evaluate the effect of Ad-MSCs, β -TCP, and ASA scaffold on bone regeneration in segmental bone defect of dogs. The previous studies suggested the clinical feasibility of ASA loaded with alveolar cells as a good alternative for bone regeneration (Gallego et al. 2010, Gallego et al. 2010). Moreover, another previous study showed that ASA scaffold with collagen I gel could provide favorable biological and mechanical environments for osteogenic differentiation of MSCs (Kang et al. 2013). Our results demonstrate that the combination of Ad-MSCs and ASA scaffold can support osteogenesis for the repair of segmental defects in long bone.

There is a controversy about the role of seeding cells in tissue regeneration. Some groups reported that scaffold alone is sufficient for bone regeneration (Clokier et al. 2002, Ueki et al. 2003). However, this study confirmed that the groups without seeding Ad-MSCs showed only a little osseous tissue formation, which could be observed from the cut edge of surrounding normal bone. This could be supported by the fact that serum-albumin scaffold loaded with Ad-MSCs in vitro had positive effect on osteogenic potential (Kang et al. 2013). It was reported that native cells with osteogenic potential could migrate into the scaffold to generate new osseous tissues and achieve bony-union in small defects (Byeon et al. 2010). However,

in critical-sized defects, either the migration rate or the amount of native cells from surrounding tissue might not be fast or sufficient enough to generate bone tissue efficiently before the degradation of scaffold, and thus it may result in scar tissue formation at the defect when scaffold alone is implanted. Our results indicate that such a mechanism is highly likely in large-sized tissue defects. Studies of using bone marrow MSCs for bone regeneration have demonstrated that seeded bone marrow MSCs could not only provide an osteogenic cell source for new bone formation, but also secrete growth factors to recruit native cells to migrate into the defect site (Bi et al. 1999, Frank et al. 2002, Harris et al. 1994). In addition, another study revealed that significant levels of cytokines released by canine umbilical cord blood-derived MSCs 1 day after implantation can enhance bone regeneration (Byeon et al. 2010). Ad-MSCs may potentiate bone matrix deposits formed under osteogenic conditions and have an osteogenic differentiation capability (Kang et al. 2012). We speculated that the acceleration of bone formation results of the present study were induced by growth factors secreted and direct osteogenic differentiation by Ad-MSCs

The selection of an appropriate scaffold material for Ad-MSCs used in bone repair remains a challenge. The scaffolds serve as temporary matrices for bone regeneration and have favorable cellular attachment, growth, and differentiation (Drosse et al. 2008). The scaffolds are physical materials of three-dimensional shape that offer an appropriate

framework and surface characteristics for adherence of MSCs, osteoblasts, osteocytes, chondroblasts, and chondrocytes (Bucholz 2002, Ishaug et al. 1997). In addition, a scaffold should be biocompatible to minimize interference with bone formation from an inflammatory reaction and should be biodegradable to match the expected rate of progressive bone replacement in the bone defect site and provide mechanical support for osteogenesis (Hutmacher 2000, Sandhu et al. 1999). MSCs combined with β -TCP showed more bone formation and osteogenic activity than those combined with any other clinically approved scaffold (Sanchez-Sotelo et al. 2000). In our previous experiment, we verified the most effective ratio of β -TCP in ectopic implantation, but this ratio may not be favorable for ASA scaffold in this present study. In the present study, the ASA scaffold with β -TCP displayed unfavorable resorption properties compared to other study (van Hemert et al. 2004). We expected that absorption of the β -TCP would have positive effect on bone formation (Byeon et al. 2010), but the groups with β -TCP showed that new bone formation hardly occurred within implant site, which are different results compared to other studies (Jang et al. 2008, Kang et al. 2012). A porous scaffold microstructure with minimal pore size ranging from 100 to 150 μm is usually required to allow tissue ingrowth (Zeltinger et al. 2001). However, it seemed that the mixed β -TCP filled up the porous structure of ASA scaffold. We surmised that it did not allow cellular penetration, extracellular matrix production, and

neovascularization.

The histologic findings confirm that ASA scaffold has favorable biocompatibility accompanying with no inflammatory reaction during experimental periods. This means that ASA scaffold could provide favorable environments for osteogenic formation like as *in vitro* (Kang et al. 2013). In addition, most areas of the middle defect sites in the treatment groups were filled with fibrous connective tissue. More time is required to verify whether fibrous tissues could be changed to osteoprogenitor cells. In conclusion, the present study suggested ASA scaffold seeded with canine Ad-MSCs accelerated new bone formation in segmental bone defects in dogs

V. References

- Arinzech, T.L., Tran, T., Mcalary, J. and Daculsi, G. (2005), "A comparative study of biphasic calcium phosphate ceramics for human mesenchymal stem-cell-induced bone formation." *Biomaterials*, 26(17), 3631-3638.
- Bi, L., Simmons, D. and Mainous, E. (1999), "Expression of BMP-2 by rat bone marrow stromal cells in culture." *Calcif Tissue Int*, 64(1), 63-68.
- Bucholz, R.W. (2002), "Nonallograft osteoconductive bone graft substitutes." *Clin Orthop Relat Res*, 395, 44-52.
- Byeon, Y.E., Ryu, H.H., Park, S.S., Koyama, Y., Kikuchi, M., Kim, W.H., Kang, K.S. and Kweon, O.K. (2010). "Paracrine effect of canine allogenic umbilical cord blood-derived mesenchymal stromal cells mixed with beta-tricalcium phosphate on bone regeneration in ectopic implantations." *Cytotherapy*, 12(5), 626-636
- Clokier, C.M., Moghadam, H., Jackson, M.T. and Sandor, G.K. (2002), "Closure of critical sized defects with allogenic and alloplastic bone substitutes." *J Craniofac Surg*, 13(1), 111-121.

- Drosse, I., Volkmer, E., Capanna, R., Biase, P.D., Mutschler, W. and Schieker, M. (2008), "Tissue engineering for bone defect healing: an update on a multi-component approach." *Injury*, 39, S9-S20.
- Ehrler, D.M. and Vaccaro, A.R. (2000), "The use of allograft bone in lumbar spine surgery." *Clin Orthop Relat Res*, 371, 38-45.
- Frank, O., Heim, M., Jakob, M., Barbero, A., Schäfer, D., Bendik, I., Dick, W., Heberer, M. and Martin, I. (2002), "Real-time quantitative RT-PCR analysis of human bone marrow stromal cells during osteogenic differentiation in vitro." *J Cell Biochem*, 85(4), 737-746.
- Gallego, L., Junquera, L., García, E., García, V., Álvarez-Viejo, M., Costilla, S., Fresno, M. F. and Meana, Á. (2010), "Repair of rat mandibular bone defects by alveolar osteoblasts in a novel plasma-derived albumin scaffold." *Tissue Eng Part A*, 16(4), 1179-1187.
- Gallego, L., Junquera, L., Meana, Á., Álvarez-Viejo, M. and Fresno, M. (2010), "Ectopic bone formation from mandibular osteoblasts cultured in a novel human serum-derived albumin scaffold." *J Biomater Appl*, 25(4), 367-381.
- Garbuz, D.S., Masri, B.A. and Czitrom, A.A. (1998), "Biology of allografting." *Orthop Clin North Am*, 29(2), 199-204.

Harris, S.E., Sabatini, M., Harris, M.A., Feng, J.Q., Wozney, J. and Mundy, G.R. (1994), "Expression of bone morphogenetic protein messenger RNA in prolonged cultures of fetal rat calvarial cells." *J Bone Miner Res*, 9(3), 389-394.

Head, W.C., Emerson Jr, R.H. and Malinin, T.I. (1999), "Structural bone grafting for femoral reconstruction." *Clin Orthop Relat Res*, 369, 223-229.

Hutmacher, D.W. (2000), "Scaffolds in tissue engineering bone and cartilage." *Biomaterials*, 21(24), 2529-2543.

Ishaug, S.L., Crane, G.M., Miller, M.J., Yasko, A.W., Yaszemski, M.J. and Mikos, A.G. (1997), "Bone formation by three-dimensional stromal osteoblast culture in biodegradable polymer scaffolds." *J Biomed Mater Res*, 36(1), 17-28.

Jang, B.J., Byeon, Y.E., Lim, J.H., Ryu, H.H., Kim, W.H., Koyama, Y., Kikuchi, M., Kang, K.S. and Kweon, O.K. (2008), "Implantation of canine umbilical cord blood-derived mesenchymal stem cells mixed with beta-tricalcium phosphate enhances osteogenesis in bone defect model dogs." *J Vet Sci*, 9(4), 387-393.

Kang, B.J., Kim, Y., Lee, S.H., Kim, W.H., Woo, H.M. and Kweon, O.K. (2013), "Collagen I gel promotes homogenous osteogenic differentiation of adipose tissue-derived mesenchymal stem cells in serum-derived albumin scaffold." *J Biomater Sci Polym Ed*, 24(10), 1233-1243.

Kang, B.J., Ryu, H.H., Park, S.S., Kim, Y., Woo, H.M., Kim, W.H. and Kweon, O.K. (2012), "Effect of matrigel on the osteogenic potential of canine adipose tissue-derived mesenchymal stem cells." *J Vet Med Sci*, 74(7), 827-836.

Kang, B.J., Ryu, H.H., Park, S.S., Koyama, Y., Kikuchi, M., Woo, H.M., Kim, W.H. and Kweon, O.K. (2012), "Comparing the osteogenic potential of canine mesenchymal stem cells derived from adipose tissues, bone marrow, umbilical cord blood, and Wharton's jelly for treating bone defects." *J Vet Sci*, 13(3), 299-310.

Kikuchi, M., Koyama, Y., Yamada, T., Imamura, Y., Okada, T., Shirahama, N., Akita, K., Takakuda, K. and Tanaka, J. (2004), "Development of guided bone regeneration membrane composed of β -tricalcium phosphate and poly (L-lactide-co-glycolide-co-epsilon-caprolactone) composites." *Biomaterials*, 25(28), 5979-5986.

Oonishi, H. (1991), "Orthopaedic applications of hydroxyapatite." *Biomaterials*, 12(2), 171-178.

Pittenger, M.F., Mackay, A.M., Beck, S.C., Jaiswal, R.K., Douglas, R., Mosca, J.D., Moorman, M.A., Simonetti, D.W., Craig, S. and Marshak, D.R. (1999), "Multilineage potential of adult human mesenchymal stem cells." *Science*, 284(5411), 143-147.

Ryu, H.H., Lim, J.H., Byeon, Y.E., Park, J.R., Seo, M.S., Lee, Y.W., Kim, W.H., Kang, K.S. and Kweon, O.K. (2009), "Functional recovery and neural differentiation after transplantation of allogenic adipose-derived stem cells in a canine model of acute spinal cord injury." *J Vet Sci*, 10(4), 273-284.

Salgado, A.J., Coutinho, O.P. and Reis, R.L. (2004), "Bone tissue engineering: state of the art and future trends." *Macromol Biosci*, 4(8), 743-765.

Sanchez-Sotelo, J., Munuera, L. and Madero, R. (2000), "Treatment of fractures of the distal radius with a remodellable bone cement a prospective, randomised study using norian srs." *J Bone Joint Surg Br*, 82(6), 856-863.

Sandhu, H.S., Grewal, H.S. and Parvataneni, H. (1999), "Bone grafting for spinal fusion." *Orthopedic Clinics of North America*, 30(4), 685-698.

Sartoris, D.J., Holmes, R.E. and Resnick, D. (1992), "Coralline hydroxyapatite bone graft substitutes: radiographic evaluation." *J Foot Surg*, 31(3), 301-313.

Schäffler, A. and Büchler, C. (2007), "Concise Review: Adipose Tissue-Derived Stromal Cells—Basic and Clinical Implications for Novel Cell-Based Therapies." *Stem Cells*, 25(4), 818-827.

Tseng, S.S., Lee, M.A. and Reddi, A.H. (2008), "Nonunions and the potential of stem cells in fracture-healing." *J Bone Joint Surg Am*, 90, 92-98.

Ueki, K., Takazakura, D., Marukawa, K., Shimada, M., Nakagawa, K., Takatsuka, S. and Yamamoto, E. (2003), "The use of polylactic acid/polyglycolic acid copolymer and gelatin sponge complex containing human recombinant bone morphogenetic protein-2 following condylectomy in rabbits." *J Craniomaxillofac Surg*, 31(2), 107-114.

van Hemert, W.L., Willems, K., Anderson, P.G., van Heerwaarden, R.J. and Wymenga, A.B. (2004), "Tricalcium phosphate granules or rigid wedge preforms in open wedge high tibial osteotomy: a radiological study with a new evaluation system." *Knee*, 11(6), 451-456.

Zeltinger, J., Sherwood, J.K., Graham, D.A., Mueller, R. and Griffith, L.G. (2006), "Effect of pore size and void fraction on cellular adhesion, proliferation, and matrix deposition." *Tissue Eng*, 7(5), 557-572.

VI. 국문초록

개의 골결손 모델에서 자가혈청유래 알부민 스캐폴드와 개 지방유래 간엽줄기세포의 골 형성 촉진

서울대학교 대학원

수의학과 수의외과학 전공

윤 대 영

이 논문은 자가골 또는 동종골 이식 대신에 전구 세포 이식 합성 골이 골절 치료를 위한 대체 방법으로 가능한지를 알아본 실험이다. 연구의 목적은 개의 결손골 모델에서 개 지방유래 간엽줄기세포 (Ad-MSCs) 주입 자가혈청 유래 알부민 (ASA) 지지체의 뼈 형성을 평가한 것이다. ASA 지지체는 가교 및 동결 건조 공정을 거쳐 만들었으며, β -TCP (Beta-tricalcium phosphate)

는 가교 공정 중에 혼합하였다. 이 후, 지방유래 간엽줄기세포를 주입하여 하루를 배양하고 이식하였다. 이식물의 조직 평가를 위해 이식 16 주 후에 채취하였다. 개는 대조군과 자가혈청유래 알부민 스캐폴드에 지방유래 간엽줄기세포와 베타-트리칼슘포스페이트의 적용 여부에 따라 4 개의 실험군으로 분류하였다. 지방유래 간엽줄기세포 주입 자가혈청유래 알부민 스캐폴드 군이 베타-트리칼슘포스페이트 적용 군들 보다 유의적인 방사선 상의 불투과성 영역 증가를 보였으며, 다른 모든 군들과 비교하여 조직 소견에서 유의적인 뼈 형성 증가를 보였다 ($p < 0.05$). 지방유래 간엽줄기세포 주입 자가혈청유래 알부민 스캐폴드는 결손골에서 골형성을 촉진시켰으며, 베타-트리칼슘포스페이트 혼합 스캐폴드는 뼈 치유와 관련한 세포의 침투를 저해한 것으로 사료된다. 또한, 섬유조직이 골전구세포로의 변환 여부를 확인하기 위해 더 많은 시간이 필요한 것으로 판단된다.

주요어: 골 결손, 지방유래 중간엽줄기세포, 혈청 유래 알부민 스캐폴드

학 번: 2011-21673